Cure Modeling and Monitoring of Epoxy/Amine Resin Systems. I. Cure Kinetics Modeling

PANAGIOTIS I. KARKANAS, IVANA K. PARTRIDGE

Advanced Materials Department, School of Industrial and Manufacturing Science, Cranfield University, Bedford, MK43 0AL, UK

ABSTRACT: The cure kinetics of four epoxy/amine systems including commercial RTM6 and F934 resins have been investigated under both isothermal and dynamic curing conditions. Differential Scanning Calorimetry (DSC) was the thermoanalytical technique used to determine the cure kinetics of these resin systems. The complexity of the cure reactions, illustrated by the results, was attributed to the variety of chemical reactions between the epoxy and the amine groups. Various cure kinetics models were implemented in order to achieve an accurate description and simulation of the cure profiles obtained from the DSC measurements in the chemically controlled region. These varied from simple *n*th order kinetic models to complicated combinations of *n*th order and autocatalytic kinetic schemes. The mathematical techniques used to evaluate the parameters of the kinetic models varied from simple linear regression to non-linear regression and peak analysis. The resulting fits were in a good agreement with the experimental results for all the resin systems and for all the experimental conditions used. © 2000 John Wiley & Sons, Inc. J Appl Polym Sci 77: 1419–1431, 2000

Key words: cure kinetics; epoxy resin; modeling; RTM6; F934

INTRODUCTION

During the cure of a thermosetting resin a number of complex chemical and physical changes occur as the material turns from a viscous liquid to a highly crosslinked solid. All these changes, which are reflected in the cure kinetics and the chemoviscosity characteristics of each individual resin system, determine the optimum set of process parameters for the production of a material that will have the best morphological and structural properties for a given application. The present study was undertaken in the context of a large, collaborative, industrial programme. It has the aim of exploring the feasibility of constructing a set of mathematical and numerical kinetic models that can be applied to the majority of epoxy resins.

To date, an extensive effort has been applied to the study of the nature of the chemical reactions that occur during the cure of thermosets and in particular of epoxy resins, as these form the majority of the resin matrices used in the aerospace composite industry.[1–4] Apart from a qualitative evaluation of the chemical processes involved in epoxy cure, a range of mathematical models has also been produced, in order to simulate the conversion advancement during the cure. These range from purely phenomenological models[5–9] to models based on the actual cure mechanism and on the evolution of the concentration profiles of all the reactive species involved.[10–13]

Despite the effort that has been expended in the exploitation of the cure kinetics of the epoxy resins, there is still no general model that can apply to the cure of all epoxy resins. The fact is that, for each epoxy resin system or at least for a family of epoxy resins, the cure kinetics of the system have to be reevaluated. Such a situation represents a severe limitation to an industrial application of any monitoring or control system requiring a quantitative knowledge of the resin cure kinetics.

Correspondence to: I. K. Partridge.

Journal of Applied Polymer Science, Vol. 77, 1419–1431 (2000)

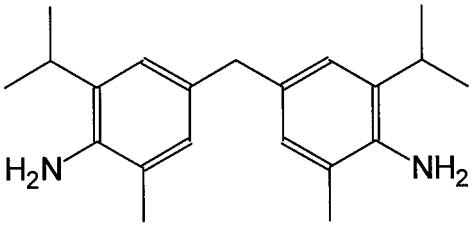

Figure 1 Structural formula of M-MIPA amine hardener.

In general, epoxy resin curing reactions involve opening of the epoxide ring followed either by a homopolymerisation reaction with further epoxide, or reaction with other curing agents to form additional products.[3] The most common procedure in curing epoxy resins is to react them with polyfunctional amines.

The basic reaction of epoxides based on diglycidyl ether of bisphenol A (DGEBA) with primary and secondary amines, in the absence of a catalyst, involves the addition of the primary and secondary amino groups of the polyamine to the epoxy group, with the simultaneous evolution of one hydroxyl group due to opening of the epoxy ring. Experimental evidence shows that the two epoxy groups of this type of resins have the same reactivity, hence these reactions proceed with the —NH amino group attacking the epoxy ring randomly. The hydroxyl groups formed by the amine/epoxide addition reaction can act as catalysts, accelerating the reaction at the early stages and exhibiting the typical course of an autocatalysed reaction. In cases where the amine is present in less than stoichiometric concentrations, further reaction of the epoxy groups with the hydroxyl groups may occur, producing an ether group.

The preparation of high performance aerospace composites involves the use of polyfunctional epoxy resins (functionality $f > 2$) in mixtures with diamines and catalysts for the acceleration of the overall reaction. Typical epoxy resins used in such applications are those based on the tetrafunctional epoxy resin tetraglycidyl-diaminodiphenylmethane (TGDDM). The most significant difference of the reaction of TGDDM with amines from that of epoxides based on DGEBA is the strong tendency of TGDDM and its derivatives to cyclisation, in contrast to DGEBA where no cyclisation occurs.[14,15]

In practice, many of the formulations incorporate catalysts to accelerate the thermal curing reaction. The two most commonly used are boron trifluoride monoethylamine, $BF_3 : NH_2C_2H_5$, and boron trifluoride piperidine, $BF_3 : NHC_5H_{10}$, complexes. Such complexes are latent catalysts at room temperature but enhance epoxide group reactivity at higher temperatures.

EXPERIMENTAL

I. Materials

Two commercially available epoxy/amine systems, RTM6 and F934, and two specially prepared experimental systems based on one epoxy resin and two amine hardeners, were used in this study.

RTM6 was supplied by Hexcel Composites (Duxford, UK) as a premixed epoxy resin system, specially developed to fulfil the requirements of the aerospace composites industry in advanced resin transfer moulding (RTM) processes.

F934 was supplied by Fiberite Europe GmBH (Germany). The general use of this resin is as matrix in composite materials and it is commercially available in several prepreg forms. Primarily it consists of a TGDDM epoxy cured with DDS hardener but also contains a boron trifluoride catalyst.[16]

The two other systems used, were produced by mixing appropriate constituents in our laboratory equipment. Both of them were epoxy/amine resin systems. The pure materials used for the preparation of those resins were one TGDDM-based epoxy resin (MY721) and two amine hardeners. The first was 4,4′-Methylenebis(2-isopropyl-6 methylaniline) (M-MIPA) with a chemical formula $C_{21}H_{30}N_2$ and molecular weight 310. This is a diamine commercially supplied by LONZA Ltd (Basel, Switzerland) under the trade name M-MIPA. The structural formula of this agent is shown in Figure 1.

The other curing agent used was 4,4′-Methylenebis (2,6-diethylaniline) (M-DEA) with the

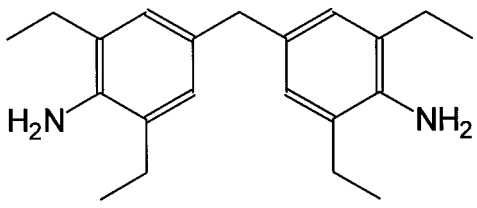

Figure 2 Structural formula of M-DEA amine hardener.

Table I Chemical Constituents of Laboratory-made Resins

Resin	pph		
	MY 721	M-MIPA	M-DEA
RMO	100	43.7	26.7
RMO2	100	70.4	—

same chemical formula as M-MIPA but with a different structural formula (see Figure 2). This agent is also supplied by LONZA Ltd. under the trade name M-DEA.

Table I shows the chemical constituents of the laboratory prepared formulations. Stoichiometric mixing ratio 0.85 : 1 between epoxy groups and amino-hydrogens was adopted for the RMO system, whereas the epoxy groups and amino-hydrogens ratio of RMO2 system was 1.

The resin mixtures were prepared according to the following procedure: after the initial melting of the hardeners at 90°C, they were dissolved into the epoxy resin at 100°C. The mixing temperature was kept stable using an oil bath. A magnetic stirrer was used throughout the 30 min mixing procedure. After mixing, the resin was kept at 80°C under vacuum for 30 minutes to remove all entrapped air and then it was free cooled to room temperature. The master batches subdivided into smaller samples, placed in individual glass containers and stored in a freezer at −18°C for further use.

II. Methods

DSC experimental data obtained on a Perkin Elmer DSC-4 apparatus apart from the isothermal measurements on RTM6 resin which were made on a Mettler Toledo 8000 apparatus. The Perkin Elmer DSC-4 was fitted with a cooler unit to achieve measurements at sub-ambient temperatures. In both instruments, a nitrogen purge gas was used to avoid any oxidation of the samples during the experiments.

IIa. Dynamic Heating Runs

Dynamic runs at constant heating rates were made in order to determine the conversion profiles and the total heats of reaction released during dynamic curing for all the resin systems used. Resin samples of 8–10 mg were encapsulated in aluminum pans and placed in the instrument furnace at ambient temperature. After cooling to −50°C and a 2 minute equilibration, the heat evolution was monitored from −50°C to 320°C using the following heating rates: 2, 5, 7.5, 10, 15 and 20°C/min.

The degree of cure, α, at any temperature T during the dynamic cure is given by:

$$\alpha = \frac{\int_{T_0}^{T_1} \frac{dH}{dT}\, dT}{\Delta H_T} \tag{1}$$

The lower bound of the integration, T_0, is the lowest temperature at which heat evolution begins. Integration of the total area enclosed under the thermogram will give the total heat of reaction released during the reaction, ΔH_T, since it is supposed that the curing reaction has proceeded to completion by the end of the run.

Integration of the above formula supposes an a priori knowledge of the baseline from which the integration has to be performed and which constitutes the sample background. The problem of sample background correction arises from the fact that the specific heat of the system continuously changes during the thermal event (e.g. curing, melting) from the level of the initial substances to that of the final product. To obtain the net effect due to the thermal event, the course of the heat capacity changes should be subtracted from the data corrected for the instrument baseline. Bandara,[17] using the thermal response of the material before and after any thermal events, constructed an expression that incorporates changes in the specific heat due to the degree of cure. This expression is given by:

$$F(t) = \frac{\int_0^t \{G(t) - F(t)\}dt}{\int_0^{t_n} \{G(t) - F(t)\}dt} \{P_2(t) - P_1(t)\} + P_1(t) \tag{2}$$

In this expression, $F(t)$ is the sample background, $G(t)$ is the total signal corrected for the instrument background and t_n is the time of termination of the thermal event. $P_1(t)$ is the DSC signal for the initial substances in the absence of any events, which can be estimated through linear extrapolation of the portion of the total curve

prior to the thermal event. $P_2(t)$ is the DSC signal from the product alone, which, for a thermoset, can be estimated by a rerun of the fully cured sample under the same experimental conditions. An iterative algorithm can be constructed to find a numerical solution for $F(t)$.

The overall reaction rate can be calculated directly from the rate of enthalpy change. Normalisation of the enthalpy rate by sample weight and division by the total heat of reaction will give the reaction rate.

IIb. Isothermal Runs

Isothermal experiments were carried out only for the RTM6 resin. Samples of 2–3 mg of the resin were encapsulated in aluminum pans and placed in the pre-heated furnace of the instrument at the isothermal temperature of the experiment. After a 2 minute thermal equilibration the measurements were started at temperatures of 140, 160, 170 and 180°C.

The degree of cure, α, at any time t during the isothermal reaction can be obtained from:

$$\alpha = \frac{\int_0^t \frac{dH}{dt}\, dt}{\Delta H_T} \tag{3}$$

where the numerator is the heat released up until time t. The baseline for the integration was estimated by drawing a horizontal line, extrapolating the baseline reached on the completion of the cure peak to the start of the peak. ΔH_T is the total heat of reaction for a completely cured sample as determined by the previously described dynamic DSC experiments. Numerical methods were used to calculate the integral of the above equation at various time intervals in order to obtain the conversion profile at each experiment. The overall reaction rates were calculated using the same method as in the dynamic case.

IIc. Residual Heat of Reaction

The conversion profiles under isothermal conditions were constructed for all resin systems by measuring the residual heat of reaction after partial cure of the resin at different time intervals at 140, 150 and 160°C. For these experiments 8–10 mg of the resin were encapsulated in an aluminium pan and placed in the pre-heated furnace of the DSC at the chosen temperature. After a 2 minute of equilibration, the time elapsed during the cure started to be recorded. When the predetermined time interval had elapsed, the sample was quenched to −50°C and subsequently scanned at a heating rate of 10°C/min until fully cured in order to determine the residual heat of reaction, ΔH_{res}.

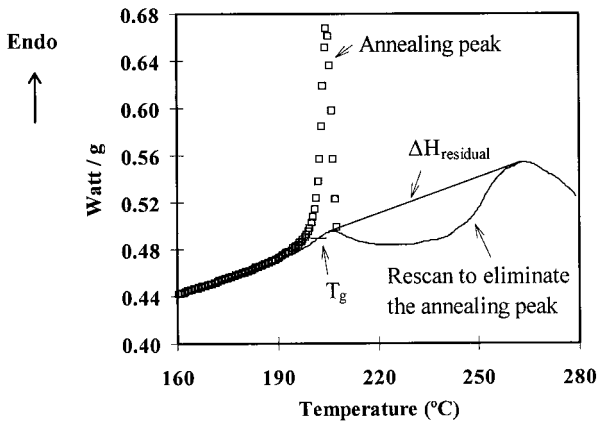

Figure 3 Endothermic physical aging peak for samples that had vitrified during cure. (a) (□) Aging peak. (b) (—) Rescan to eliminate the physical aging peak. The T_g of the partially cured resin is also shown as the midpoint of the endothermic shift in the thermogram.

The corresponding degree of conversion, α, was given by:

$$\alpha = \frac{\Delta H_T - \Delta H_{\text{res}}}{\Delta H_T} \tag{4}$$

The above procedure was repeated, using different samples, for a range of time intervals and temperatures, until enough points had been determined to enable the construction of the conversion-time profiles. The corresponding reaction rates were determined by numerical differentiation with respect to time of the experimentally obtained conversion-time dependence. Some samples showed a characteristic spike in the thermogram just before the exotherm started, which was attributed to physical aging of the resin. When the resin has passed the vitrification point, a subsequent dynamic scan of that resin usually shows an endothermic spike in the vicinity of the T_g, as can be seen clearly in the thermogram of Figure 3. To eliminate this sub-T_g physical annealing, the specimens were quenched rapidly from temperatures just above the endothermic peak to the temperature of −50°C. The subsequent re-heating of the specimens using the same experimental con-

Table II Total Heats of Reaction of Resin Systems at Different Heating Rates

Resin System	Heating Rate (°C/min)						Average ΔH_T (J/g)
	2	5	7.5	10	15	20	
	Total Heat of Reaction ΔH_T (J/g)						
RTM6	432	437	440	431	437	438	436
RMO	478	473	480	477	495	476	480
RMO2	443	451	452	446	456	454	450
F934	450	447	449	452	449	452	450

ditions was free of the endothermic peak (Figure 3). This method, also used by Gillham and coworkers,[8] results in an error introduced by the cooling and the subsequent re-heating of the specimens of not more than 1–2°C in terms of the final T_g value of the cured resin.

RESULTS AND DISCUSSION

I. Heating Rate Effects

Initially, the total heats of reaction, ΔH_T, were determined for all the epoxy-amine systems used in this study. To check if the reaction mechanism changes with the heating rate used, the dynamic DSC runs were repeated at heating rates of 2, 5, 7.5, 10, 15 and 20°C/min.

It is evident from results shown in Table II that the total heat of reaction remains constant for each of the resin systems, over this range of heating rates. This observation might suggest that the reaction mechanism remains constant at constant heating rates in the range between 2 and 20°C/min, although differences in the three dimensional network formed during the cure provides evidence for the contrary. In the following sections, an average value of the total heat of reaction will be used for each resin system. These average values are given in Table II. Typical DSC dynamic run thermograms are shown in Figure 4 for the RTM6 resin system. As might be expected, curing of the resin at low heating rates has as a result a drop of the onset of the reaction to lower temperatures. This effect is observed throughout the cure for all these resin systems; at a specific temperature, the degree of cure is higher at lower heating rates. More information can be extracted if we consider the reaction rate as a function of the degree of cure normalised by the maximum reaction rate attained at each heating rate. Such plots are shown in Figure 5 for the RMO resin system. It is evident from this figure that all the plots fall onto a master curve up to around 60% conversion where higher heating rates start to deviate slightly upwards, showing higher reaction rates. This master curve provides strong evidence that the reaction mechanism does not change significantly with different heating rates. The same trend is followed for all the resin systems used here, except for the F934 resin.

In Figure 6 the reaction rates are plotted as functions of temperature for this system. A constant reaction rate is observed for all heating rates in a limited conversion window in the low conversion area. The conversion range for which this plateau is observed drops to lower conversions for lower heating rates, indicating that the heating rate does affect the reaction mechanism

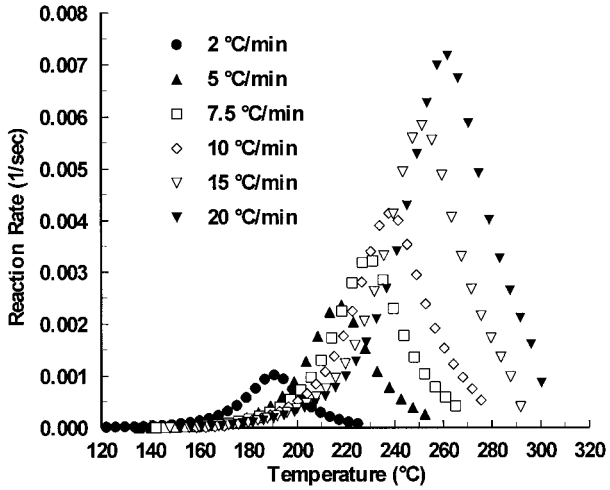

Figure 4 Evolution of reaction rates with temperature during dynamic cure of RTM6 resin at constant heating rates. Experimental results from DSC scans.

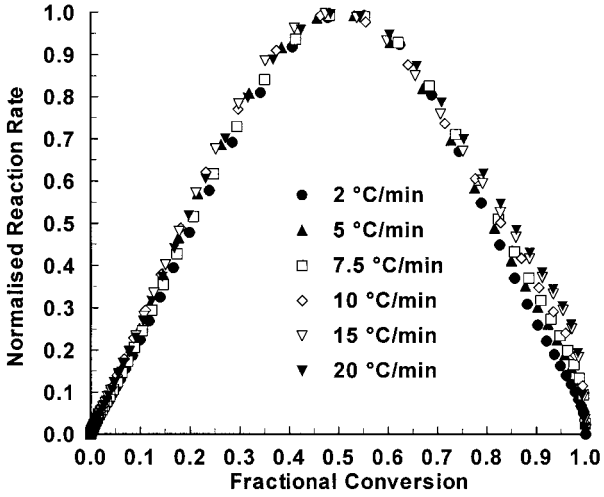

Figure 5 Reaction rates normalized by the maximum reaction rate as a function of fractional conversion for the RMO resin system, for dynamic cure at different heating rates. Experimental results from DSC scans.

for this particular resin system. This system is discussed further in sub-section III.b.

II. Chemically Controlled Cure Kinetics Under Isothermal Conditions

IIa. RTM6, RMO and RMO2

Cure kinetics modeling was first carried out for the case of isothermal cure. The most frequently used kinetic model of epoxy cure, is the autocatalytic model,[18] given by Eq. 5:

$$\frac{d\alpha}{dt} = (k_1 + k_2\alpha^m)(1 - \alpha)^n \qquad (5)$$

where:

$\frac{d\alpha}{dt}$ = reaction rate
k_1 and k_2 = reaction rate constants following an Arrhenius temperature dependence
α = fractional conversion
m and n = reaction orders

This model was applied to the isothermal cure of all our resin systems apart from the F934 resin, which is a catalysed system and does not show any autocatalytic phenomena. The modeling was applied up to approximately 55–60% conversion. At this level of conversion, the resin is still in the chemically controlled region and there is no strong effect from diffusion phenomena.

Two parameter evaluation procedures were used. The first one is the well known Ryan-Dutta method,[18] which is based on the two characteristic points of the isothermal reaction rate: the initial and the maximum reaction rates. The second method is based on Eq. 6 obtained by a suitable rearrangement and algebraic manipulation of Eq. 5. For an isothermal situation, a plot of the left hand side of Eq. 6 with respect to ln α will give a straight line with slope m and an intercept of ln k_2. The reaction rate constant k_1 can be determined by the values of the initial reaction rates, as in the Ryan-Dutta method.

$$\ln\left(\frac{\frac{d\alpha}{dt}}{(1-\alpha)^{r-m}} - k_1\right) = \ln k_2 + m \ln \alpha \qquad (6)$$

Here r is the reaction total order. Results of the application of the two methods to isothermal experiments for the RTM6, RMO and RMO2 resin systems are given in Table III.

Although the results for both methods indicate that the use either of them will give essentially the same prediction, the computation effort that is needed to reach those results is different in the two cases. Care has to be taken during the construction of the straight lines for the second method, since the initial points from the DSC data tend to destabilize the results. The same problem was observed by Kenny[19] who also implemented this technique for the evaluation of the

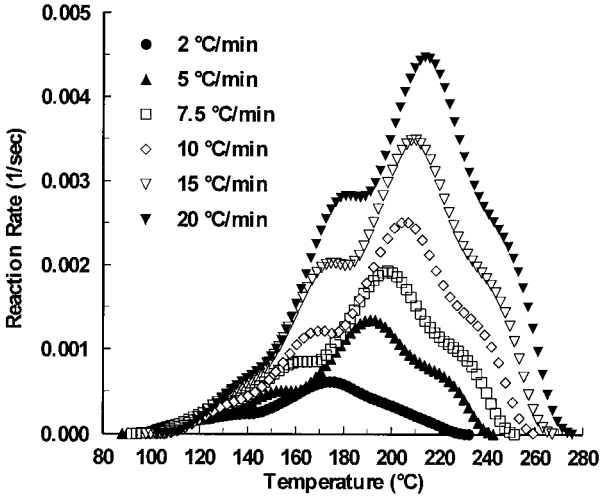

Figure 6 Evolution of reaction rates with temperature during dynamic cure of F934 resin at constant heating rates. Experimental results from DSC scans.

Table III Comparison of Ryan–Dutta and Present Methods for the Computation of the Parameters of the Model Given by Eq. (5) and DSC Results for the Cure of RTM6, RMO, and RMO2 Resins Under Isothermal Conditions

Method	r	m	n	E_1 (kJ/mol)	A_1 (min^{-1})	E_2 (kJ/mol)	A_2 (min^{-1})
				RTM6 resin			
Ryan–Dutta	2.5	1.216	1.284	74.69	4.5×10^6	58.37	1.3×10^6
Present	2.5	1.202	1.298	74.69	4.5×10^6	59.18	1.6×10^6
				RMO Resin			
Ryan–Dutta	2.5	1.192	1.308	78.44	1.3×10^7	57.88	9.1×10^5
Present	2.5	1.278	1.222	78.44	1.3×10^7	56.14	5.6×10^5
				RMO2 Resin			
Ryan–Dutta	2.5	1.300	1.200	75.54	6.1×10^6	53.08	2.7×10^5
Present	2.5	1.313	1.187	75.54	6.1×10^6	54.68	4.3×10^5

kinetic parameters. For that reason, it is better to construct the lines for conversions well into the cure. The accuracy of the second method is likely to be better since it takes into account all the experimental data, whereas the Ryan-Dutta method uses only the initial and maximum points, disregarding what happens in between.

A close look at Table III reveals the similarity of the cure kinetics for the three resin systems. Comparable values have been evaluated for all the kinetic parameters. The activation energies fall in the same range of values deviating only 2–3 kJ/mol from the average values of about 76 kJ/mol for the non-catalytic reaction, E_1, and 56 kJ/mol for the catalytic reaction, E_2. The same trend is observed for the reaction orders. All resin systems follow the same total order, r, of 2.5 with the partial reaction orders being about the half of the total order. The similarity of the activation energies is indicative of the similarity of the reaction mechanism. All three resins are epoxy/amine systems, thus the main reactions during the cure should be the same for all of them. Deviation of the conversion profiles of these resin systems between each other is reflected in the different pre-exponential Arrhenius factors, A_1 and A_2, obtained during the evaluation procedure. The relative weight of each reaction to the total reaction is different for each resin system, is proportional to the pre-exponential factor and depends on the individual chemical constituents used. Thus, although the epoxy resin used is the same (TGDDM), the use of two different amine hardeners means that a change in their relative concentrations, is likely to favour some reactions more than others.

The goodness of the fit of the above constructed models with the experimental results is shown in Figure 7 for all the 'RTM6-type' resin systems, for an isothermal cure at 140°C. Since at this stage the models do not compensate for the diffusion phenomena that are expected to occur as the resin passes from the rubbery to the glassy state, the

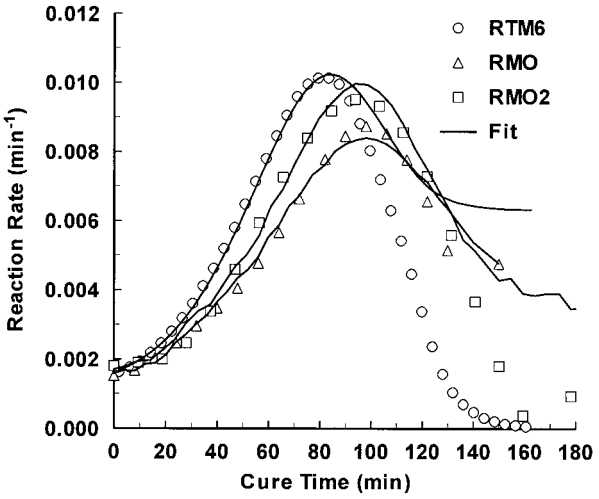

Figure 7 Reaction rate versus cure time of RTM6, RMO, and RMO2 resins under isothermal cure at 140°C. Symbols indicate experimental data, whereas solid lines indicate fits of eq. (5) with parameters evaluated by the Ryan–Dutta method given in Table III.

Table IV Kinetic Parameters for *n*th-Order Kinetics [Eq. (7)] of F934 Resin Cure Under Isothermal Conditions

Temperature (°C)	T^{-1} (K^{-1})	k (s^{-1})	ln k
130	0.002481	0.006035	−5.1102
140	0.002421	0.009719	−4.63367
150	0.002364	0.01747	−4.04725
160	0.002309	0.027192	−3.60484

Kinetic Parameters		
n	A (s^{-1})	E (kJ/mol)
0.298	2.34×10^7	74.03

fits start to deviate from the experimental data for conversions of approximately 50%.

IIb. F934 Resin System

The reaction mechanism of the F934 resin system is different from the reaction mechanism followed by the other resin systems. This is due to the fact that F934 resin contains catalysts which accelerate the epoxy-amine and epoxy-epoxy reactions in various ways. The catalytic nature of the reaction should, in principle, give rise to non-OH-catalysed reactions. For that reason, a simple nth order reaction scheme (Eq. 7) was first applied to the isothermal experimental data of F934 resin.

$$\frac{d\alpha}{dt} = k(1-\alpha)^n \tag{7}$$

For a reaction that follows nth order kinetics, integration of the reaction rate under isothermal conditions will give:

$$\frac{(1-\alpha)^{n-1}-1}{n-1} = kt \tag{8}$$

A plot of the left hand side of Eq. 8 against the cure time t will give a straight line with slope k. These plots were constructed for the three temperatures used in this investigation. The reaction order n was varied until a straight line with the highest correlation coefficient r^2 had been achieved. Combined results from all the isothermal experimental data were used in order to calculate a unique reaction order for all the cure temperatures. Data manipulation was made for levels of conversions up to 50% in order to avoid interference with diffusion at the later stages of the cure. The computed kinetic parameters of the isothermal cure of F934 resin are given in Table IV and the resulting fits in Figure 8.

Comparison of the evaluated parameters with the ones obtained for the cure of the other three resin systems (see Table III and Table IV), shows that there is a very good agreement between the activation energy of the cure reaction of F934 resin and the activation energy of the non-catalysed epoxy/amine addition reaction of RTM6, RMO and RMO2 resin systems. This observation suggests that the catalyst in the F934 resin favours the non-OH-catalysed reactions.

This catalysis is reflected in the reaction rate profiles of F934 resin (see Figure 8). As can be seen in this figure, a continuous decrease in the reaction rate at all cure temperatures is observed. This suggests that the autocatalytic behaviour is masked during the isothermal cure of F934 resin. The fit of the nth order kinetics model can also be seen in the same figure. The agreement between experimental data and model prediction is very good up to conversion of 50%, where deviation starts to appear because of diffusion limitations.

III. Cure Kinetics Under Dynamic Curing at Constant Heating Rates

IIIa. RTM6, RMO and RMO2

In the previous section the kinetics models for the RTM6, RMO and RMO2 resin systems were es-

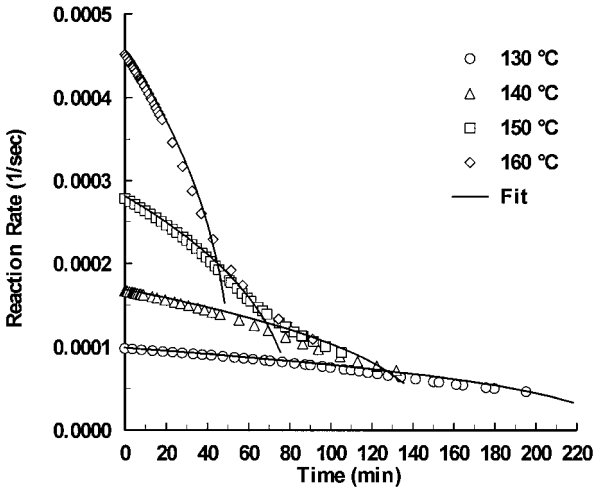

Figure 8 Reaction rate during isothermal cure of F934 resin at various cure temperatures.

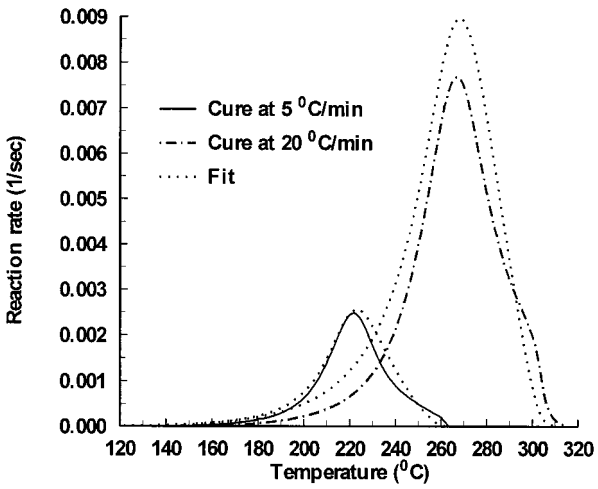

Figure 9 Dynamic cure of RMO resin at various heating rates. Fit was made using eq. (5) and the parameters calculated by the Ryan–Dutta method (Table III).

tablished for curing under isothermal conditions. Application of the same models to the dynamic cure of these resins is guaranteed to fail a priori because of the narrow temperature range for which the kinetic parameters have been evaluated, the empirical nature of the kinetic model and possible changes in the reaction mechanisms.

The failure of the model is demonstrated in Figure 9, where the cure of RMO resin under dynamic conditions at 5 and 20°C/min has been simulated with the kinetic parameters evaluated by the Ryan-Dutta method, as given in Table III. Although the fit of the model is reasonably good for the low heating rate of 5°C/min, probably because of the limited temperature window that is followed for this cure, the fit is well deviated for the 20°C/min cure, especially in the area of the maximum reaction rate.

A re-evaluation of the kinetic parameters of the model of Eq. 5 is needed to achieve a better fit. The two methods described in the previous section for the isothermal cure are not applicable; both these methods treat the reaction rate constants as unchanged throughout the cure, which is true under isothermal conditions, as these are functions only of temperature. Under dynamic cure, at each point into the cure, the rate constants will have a different value, since the temperature is changing. For this reason some other technique has to be used for the kinetic parameters evaluation. In this study the kinetic parameters were evaluated using non-linear regression analysis on the combined experimental data of all the heating rates used. The details of the computational method are available elsewhere.[20] The activation energies computed for isothermal curing were kept unchanged, whereas the rest of the parameters were varied until the best fit had been achieved. The set of the parameters that minimised the sum of the squared differences between experimental reaction rates and predicted reaction rates was taken as the model-estimated set of parameters. The evaluated parameters are given in Table V and the goodness of the fit is shown in

Table V Kinetic Parameters Evaluated by Nonlinear Regression Analysis for the Dynamic Cure of RTM6, RMO, and RMO2 Resins

Kinetic Model [Eq. (5)]						
Resin	A_1 (s^{-1})	E_1 (kJ/mol)	A_2 (s^{-1})	E_2 (kJ/mol)	m	n
RTM6	1.68×10^4	74.69	2.15×10^4	58.37	0.869	1.390
RMO	2.51×10^5	78.44	1.42×10^5	57.88	1.204	1.656
RMO2	8.57×10^3	75.54	6.77×10^4	53.08	1.268	1.521

Kinetic Model [Eq. (9)]							
Resin	A_1 (s^{-1})	E_1 (kJ/mol)	A_2 (s^{-1})	E_2 (kJ/mol)	m	n_1	n_2
RTM6	2.60×10^4	74.69	5.78×10^4	58.37	1.217	0.449	1.786
RMO	4.24×10^4	78.44	2.13×10^5	57.88	1.668	0.519	2.221
RMO2	1.13×10^4	75.54	9.04×10^4	53.08	1.495	0.449	1.845

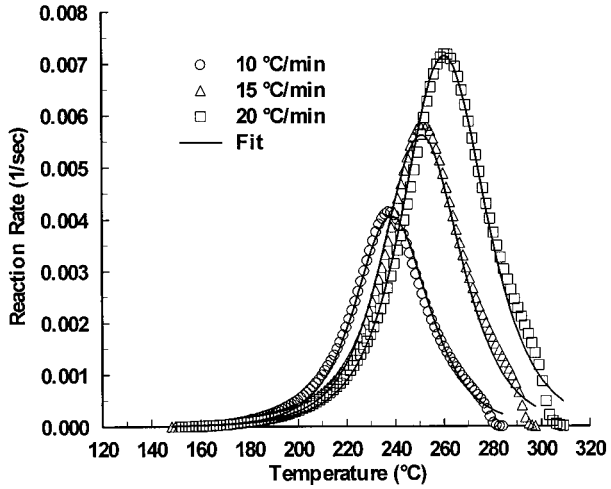

Figure 10 Cure kinetics simulation of RTM6 resin under dynamic conditions. Equation (5) was used for the fit, with the parameters given in Table V.

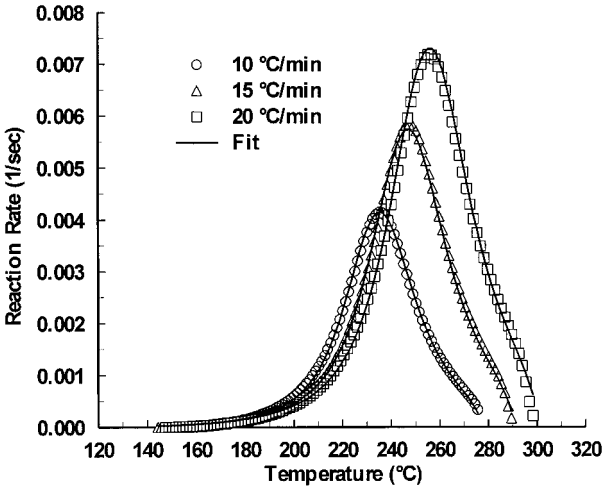

Figure 11 Cure kinetics simulation of RTM6 resin under dynamic conditions. Equation (9) was used for the fit, with the parameters given in Table V.

Figure 10 for the dynamic cure of the RTM6 resin at various heating rates.

Comparison between the experimental data and the model prediction shows very good agreement over almost the whole range of the cure, apart from the end of the cure where some deviation is observed. This observation suggests a need for a further modification of the model in order to fit the experimental data accurately throughout the cure.

A suitable modification has been found to be given by the expression[21]:

$$\frac{d\alpha}{dt} = k_1(1-\alpha)^{n_1} + k_2\alpha^m(1-\alpha)^{n_2} \qquad (9)$$

Application of the modified model, following the same evaluation procedure of non-linear regression, resulted in the fit shown in Figure 11 for the RTM6 resin system. The kinetic parameters used for the fits are given in Table V. The fits that were obtained by the modified model show a very good agreement with the experimental results throughout the cure and at all heating rates, justifying the use of Eq. 9 as the most appropriate cure kinetics model for these resin systems.

IIIb. F934 Resin

The plots of the reaction rate during dynamic cure of this resin, as presented in Figure 6, show the appearance of multiple peaks. This suggests that a multiple activated reaction mechanism is followed during curing. The consistency of the reaction mechanism throughout the range of the heating rates used was checked prior to any modeling attempts. The reaction rates, normalised by the maximum reaction rate attained at each heating rate, were plotted as functions of the fractional conversion, in Figure 12. As can be seen in this figure, there exists a master curve that describes the changes in the reaction rates with conversion, apart from the low conversion area, where this correlation breaks down. This is consistent with the idea of several reactions occurring simulta-

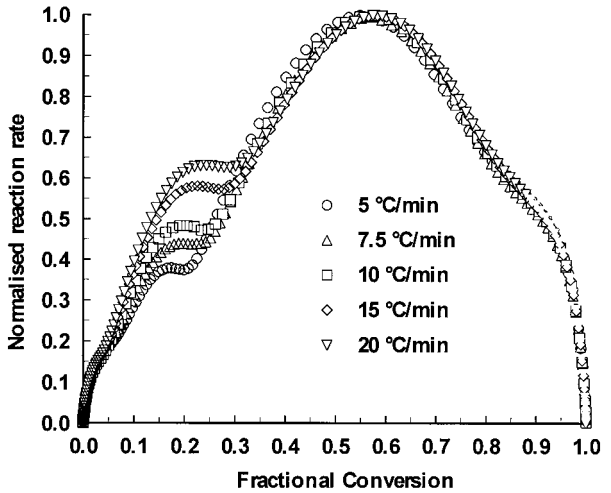

Figure 12 Normalized reaction rate over the maximum reaction rate as a function of the degree of conversion of the dynamic cure of F934 resin at various heating rates.

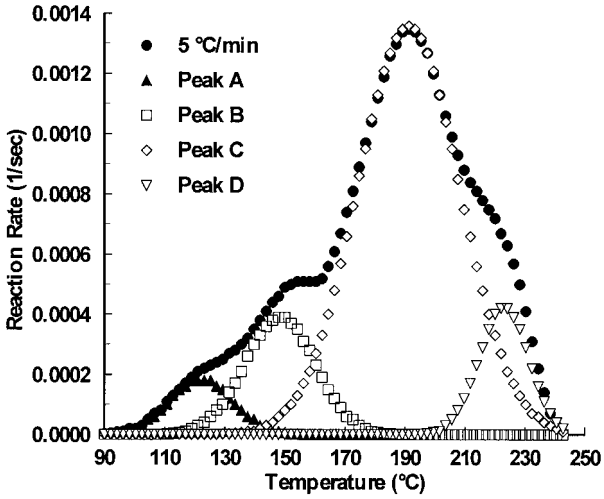

Figure 13 Peak separation of the reaction rate profile of F934 resin under dynamic cure at 5°C/min. Four peaks were identified using the Gaussian distribution function.

neously, the relative proportions of the individual reactions being dependent upon the length of time for which the resin system is exposed to any given temperature range.

In order to have an indication of the relative weight of each reaction to the overall reaction rate and to identify which reaction is responsible for the break down of this master curve, peak separation was applied to the experimental data of the dynamic cure of the F934 resin. A Gaussian distribution was applied for the peak separation and the number of peaks was limited to four.[20] The results of peak analysis at heating rate of 5°C/min can be seen in Figure 13. In order to examine the relative weights of each peak, the peak heights were normalised by the peak height of Peak C. The evaluated parameters of the Gaussian distribution of each peak at all heating rates are shown in Figure 14 as plots of normalised peak heights against heating rate. Close examination of these results shows that Peaks A, C, D give the same contribution to the overall reaction rate at all heating rates, whereas Peak B has a variable contribution. The weight of Peak B increases as the reaction rate increases, indicating that the reaction mechanism that is hidden under that peak depends on the heating rate. This observation matches the previous observation of the break down of the master curve in Figure 12. The conversion range where the down break was observed is in the temperature range of Peak B.

The results obtained from the peak analysis were further used to obtain the cure kinetics of F934 resin. The temperature dependence of each peak at all heating rates was investigated. The method used was the Ozawa method[22] given by Eq. 10. In this expression, β is the heating rate, T_m is the temperature at peak and A, E are the Arrhenius parameters.

$$\ln\left(\frac{\beta}{T_m^2}\right) = \ln\left(\frac{AR}{E}\right) - \log\left[\frac{ART_m^2}{\beta E}\exp\left(-\frac{E}{RT_m}\right)\right] - \frac{E}{RT_m}\frac{1}{} \quad (10)$$

Application of Eq. 10 to the peak temperatures gave the activation energies and the preexponential factors for each peak, thus the Arrhenius parameters of the reaction rate constants for each reaction mechanism responsible for each peak were evaluated.

The Arrhenius parameters for each reaction are given in Table VI. From the above analysis it follows that the overall reaction rate for the dynamic cure of the F934 resin can be written as a sum of four individual reaction rates, one for each peak identified previously. Using a simple nth order reaction scheme for each individual reaction, the overall reaction rate is written:

$$\left.\frac{d\alpha}{dt}\right|_{\text{Total}} = \sum_{i=1}^{4} W_i k_i (1-\alpha_i)^{n_i} \quad (11)$$

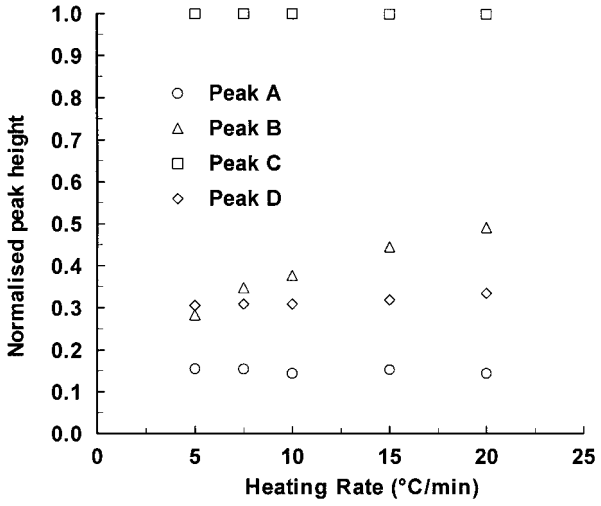

Figure 14 Peak-separation results of reaction rate of F934 resin cured under dynamic conditions at various heating rates. Peaks normalized by the height of peak C.

Table VI Kinetic Parameters Evaluated by Nonlinear Regression Analysis for the Dynamic Cure of F934 Resin

Arrhenius Parameters	Reaction A	Reaction B	Reaction C	Reaction D
E_i (kJ/mol)	88.11	79.16	102.42	102.93
A_i (s^{-1})	2.15×10^9	2.64×10^7	1.55×10^9	2.81×10^8
n_i	0.617	0.560	1.094	0.644
W_i	0.035	—	0.586	0.255
Relative Weight Factor W_2 for Reaction B				
$W_2 = 0.0302 + 0.04 \ln(\beta)$				

where W_i is the relative weight of each reaction rate to the total. In order to evaluate the parameters of this model, the same non-linear regression technique was used as with the previously described models. The Arrhenius parameters in Table VI were used in this model to evaluate the rest of the parameters, namely reaction orders n_i and relative weights W_i.

The results were evaluated from the combined experimental reaction rates at all heating rates with the same non-linear regression analysis procedure. The evaluated parameters are shown in Table VI. Variation of the relative weight of reaction 'B' was allowed, as this had been found to change with changing heating rate. The relative weight W_2 was found to change linearly with the natural logarithm of the heating rate.

The fit of the model given by Eq. 11 with the kinetic parameters in Table VI is shown in Figure 15 for the dynamic cure of F934 resin at 5°C/min. The individual reaction rates of the constituent reactions are shown in the same figure as separate plots.

CONCLUSIONS

A detailed calorimetric study of the reaction kinetics of four epoxy/amine resin systems was carried out in this study. The key issues identified from the results concerning the cure mechanisms of the resins were: (i) complex reaction mechanisms for all resins; (ii) constant cure mechanism for all the resins apart from the cure of the catalyst containing resin F934, which showed indications of changes in the reaction mechanism in cures at different heating rates; (iii) autocatalytic phenomena for the resin systems not containing catalysts (RTM6, RMO and RMO2) and; (iv) diffusion phenomena for all the isothermal cure cycles, leading to incomplete curing.

Several modeling techniques were applied, based on information on the reaction mechanisms characteristics of each individual resin. A number of phenomenological models derived for a simple epoxy/amine cure were used. Irrespective of the nature of the kinetic model, the activation energies that were estimated revealed that three of the four resin systems investigated (RTM6, RMO and RMO2) follow the same reaction mechanism. Some variability was observed in the values of the calculated kinetic parameters such as the preexponential factors of the reaction rate constants. This is more likely to be a direct effect of the

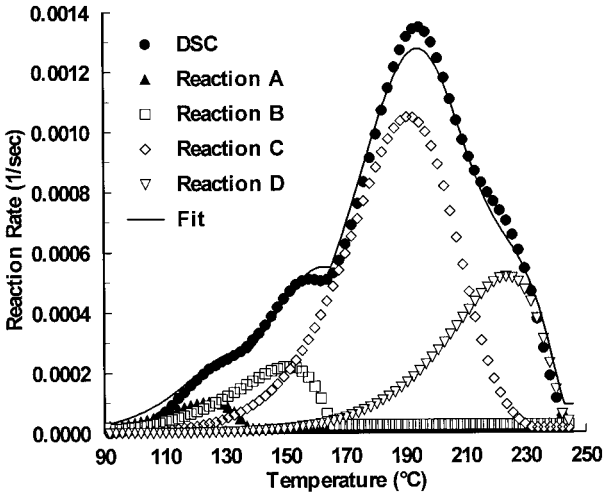

Figure 15 Kinetic modeling of F934 resin cured under dynamic conditions at 5°C/min. Equation (11) was used for the fit with the kinetic parameters shown in Table VI.

stoichiometry differences, leading to different contributions from individual reaction types, rather than any intrinsic differences in the overall reactions mechanisms.

Assumptions of simple reactions of the epoxide groups with the amines were found to be adequate to describe mathematically the cure kinetics of all these resins. The use of both autocatalytic and non-autocatalytic reaction schemes in the models was able to describe the two activation mechanisms that are followed during the cure reaction for the resins not containing any catalysts. The autocatalysis was attributed to the hydroxyl groups produced during the epoxy/amine reaction. For the F934 resin, which contained BF_3 catalysts, a simple nth order reaction mechanism was found sufficient to describe the cure kinetics under isothermal conditions.

The cure kinetics under dynamic conditions were found to be more complex to model. A modified model was used to fit the experimental data of the cure kinetics under dynamic conditions. In the case of the F934 resin, a peak separation technique was needed to identify the individual reaction contributions observed in the DSC thermograms. Further modeling of each individual reaction step was implemented by the use of a simple nth order reaction mechanism.

The fitting of the models obtained was highly satisfactory for all the resins investigated. The study demonstrated the methodology and modeling efforts required to obtain accurate cure kinetics models for these types of epoxy resins. From an industrial view point, the need for at least some knowledge of the chemical compounds of the resin to be modelled represents a significant drawback. A search continues for an alternative means of cure kinetics modeling, giving perhaps less accurate results, but requiring less effort. A possible alternative method will be the subject of a further communication.

The authors acknowledge financial support for PIK by the industrial partners in DTI/EPSRC LINK Structural Composites project ('PORPPC' GR/J96222), namely ShortBrothers plc, British Aerospace plc and DERA Farnborough. Helpful discussions with Fiberite (Europe) and with Dr. D. Attwood are also gratefully acknowledged.

REFERENCES

1. Lee, H.; Neville, K. Handbook of Epoxy Resins, McGraw-Hill, New York, 1967.
2. Smith, I. T. Polymer 1961, 2, 95.
3. Ellis, B. Chemistry and Technology of Epoxy Resins, Blackie Academic & Professional, Chapman & Hall, Glasgow, 1993.
4. Flory, P. J. Principles of Polymer Chemistry, Cornell University Press, Ithaca, New York, 1953.
5. Barton, J. M. Advances in Polymer Science 1985, 72, 111.
6. Horie, K.; Hiura, H.; Sawada, M.; Mita, I.; Kambe, H. J Polym Sci: Part A-1 1970, 8, 1357.
7. Prime, R. B. Polym Eng & Sci 1973, 13, 365.
8. Wisanrakkit, G.; Gillham, J. K. J Appl Polym Sci 1990, 41, 2885.
9. Kenny, J. M.; Trivisano, A. Polym Eng & Sci 1999, 31, 1426.
10. St. John, N. A.; George, G. A. Polymer 1992, 33, 2679.
11. Dusek, K. Advances in Polymer Science 1986, 78, 1.
12. Gupta, A. M.; Macosko, C. W. J Polym Sci: Part B: Polym Phys 1990, 28, 2585.
13. Riccardi, C. C.; Williams, R. J. J Polymer 1986, 27, 913.
14. Matejka, L.; Spacek, P.; Dusek, K. Polymer 1991, 32, 3190.
15. Johncock, P.; Tudgey, G. F.; Cunliffe, A. V.; Morell, R. K. Polymer 1991, 32, 323.
16. Morgan, R. J.; Mones, E. T. J Appl Polym Sci 1987, 33, 999.
17. Bandara, U. J Therm Anal 1986, 31, 1063.
18. Ryan, M. E.; Dutta, A. Polymer 1979, 20, 203.
19. Kenny, J. M. J Appl Polym Sci 1994, 51, 761.
20. Karkanas, P. I. "Cure Modeling and Monitoring of Epoxy/Amine Resin Systems," PhD Thesis 1998, Cranfield University, UK.
21. Karkanas, P. I.; Partridge, I. K.; Attwood, D. Polymer International 1996, 41, 183.
22. Ozawa, T. J Therm Anal 1970, 2, 301.